Archival Report

Biological Psychiatry: CNNI

Thalamic Nuclear Volumes in Fetal Alcohol Spectrum Disorders: From Adolescence to Middle-Age Twenty Years Later

Adolf Pfefferbaum, Edith V. Sullivan, Manojkumar Saranathan, Kilian M. Pohl, Amanda Bischoff-Grethe, Susan A. Stoner, and Edward P. Riley

ABSTRACT

BACKGROUND: Midline orofacial and brain structures, including the multinucleated thalamus, may be differentially sensitive to prenatal alcohol exposure and vulnerable to accelerated aging.

METHODS: Two sets of magnetic resonance imaging (MRI) data separated by 20 years are reported for control individuals, individuals with fetal alcohol syndrome (FAS), and nondysmorphic individuals with heavy fetal alcohol exposure (FAE). MRI1 included 179 participants, with 69 participants reassessed at MRI2. Segmentation produced estimates of bilateral thalamic volume and 10 bilateral nuclei, which were aggregated into anterior, ventral, posterior, and medial volumes. Differences were assessed with and without correction for intracranial volume (ICV).

RESULTS: MRI1 revealed stepwise group differences in ICV, total thalamic volume, and anterior and ventral regions uncorrected for ICV, where control > FAE > FAS. Corrected for ICV, the smaller volumes persisted in the anterior and ventral regions, although differences between the FAE and FAS groups were attenuated. Nuclei volumes were selectively smaller in the alcohol-exposed groups than in the control group even after controlling for ICV. Longitudinally, thalamic volumes typically declined over time, maintaining the stepwise effects and with little evidence for accelerated decline in the FAE or FAS groups.

CONCLUSIONS: These novel data revealed stable deficits in thalamic nuclei of the groups with heavy prenatal alcohol exposure. After 20 years, the deficits persisted but without accelerated age-related decline and following the same aging pattern as control individuals. Despite parallel aging functions in all groups, ICV adjustment yielded volume deficits localized to the anterior and ventral thalamic nuclei, differing from patterns in the remaining thalamic nuclei and cortical brain structures.

https://doi.org/10.1016/j.bpsc.2025.04.002

Fetal alcohol spectrum disorders (FASDs) represent a leading preventable cause of cognitive impairment and functional disability and have been identified in approximately 5% of U.S. children in the first grade (1). Stemming from harm to the central nervous system during its early development, fetal alcohol-induced impairments are long lasting, limiting opportunities for education and employment, independent living, and other desirable activities of daily life [reviewed in (2)]. FASD and its various diagnostic forms, including fetal alcohol syndrome (FAS), partial FAS, alcohol-related neurodevelopmental disorder, alcohol-related birth defects, and neurobehavioral disorder associated with prenatal alcohol exposure, encompass the physical, cognitive, and behavioral abnormalities caused by significant prenatal alcohol exposure (PAE) (https://www.niaaa.nih.gov/publications/brochures-and-fact-sheets/understanding-fetal-alcohol-spectrum-disorders). The study of brain structure has the potential to localize neural mechanisms possibly permanently damaged that underlie impairment in contrast to those escaping the throes of PAE that contribute to unaffected abilities.

Selective facial features of individuals with PAE are physiognomic associates of anomalous development of midline brain structures (3–5). However, it remains controversial whether volume deficits of midbrain structures endure when adjusted for pervasive intracranial volume (ICV) deficits that characterize individuals with FASD [reviewed in (2,6)]. The thalamic volume deficit may be especially relevant in FASD given its midline location and its relationship to greater dysmorphology of the philtrum (7). Although an enduring thalamic deficit despite ICV correction has been noted in different samples of individuals with FASD (8–11), others found that ICV adjustment either significantly attenuated or fully accounted for thalamic volume deficits in FASD (7,12,13). Notably, these studies volumed the whole thalamus despite its multinucleated structural complexity (14–16), raising the possibility that the thalamic nuclei may be differentially affected by PAE and have differential relationships with ICV and orofacial dysmorphology.

The thalamus comprises more than 60 nuclei, which are beyond the segmentation capabilities of current neuroimaging

ISSN: 2451-9022

resolution. Nonetheless, analytical developments now enable reliable measurement of aggregated thalamic regions and nuclei (17,18) using postprocessing algorithms applied to standard T1-weighted magnetic resonance imaging (MRI) (19,20). The thalamus is likely to have functional relevance to FASDs given that different regions of the thalamus serve differential roles in sensory, motor, cognitive, and emotional functions, each of which can be adversely affected in FASDs [reviewed in (2,21)].

Whether PAE exerts differential aging effects on thalamic regions remains unknown and requires longitudinal investigation of regional brain volumes into adulthood [cf. (22,23)]. Most longitudinal MRI studies reported to date have been conducted with children and adolescents and span only 2 to 5 years of follow-up [e.g., (24,25)]. One such study measured volumes of the brain and subcortical structures, including the whole thalamus. At the initial MRI, the thalamic volume of the FASD group was 14% smaller than that of the control group. Approximately 2 to 4 years later, the thalamus did not change significantly in volume in either group even though the FASD volume had increased 2.4%, whereas the control volume had decreased 2.1%. Notably, the FASD thalamic volume deficit endured after correcting for total brain volume (11). Persistence of a thalamic volume deficit after ICV correction was also reported in a cross-sectional study (26).

Perhaps the longest follow-up study measured MRI-derived brain volumes after a 20-year span, from a mean age of approximately 20 to 40 years, and surveyed the whole supratentorial volume with a focus on cortical lobar regions and white matter structures. Declines in cortical volumes in control, FAE (the term used at the time of the original scan to designate an individual who had been exposed to high amounts of alcohol prenatally but who did not meet full criteria for FAS), and FAS groups emerged contemporaneously with increases in white matter volumes in all groups, consistent with the continuing developing brain from adolescence through adulthood (27,28). Despite these age-related changes in volumes, all 3 groups showed similar developmentally related levels of cortical gray matter decline and white matter increases while maintaining diagnostically related stepwise volume effects: control > FAE > FAS (28). Although that study did not report on thalamic volume, those longitudinal MRI data remained available to pursue the current question about the potential of a pattern of accelerated aging across thalamic regions and nuclei of individuals with FASD.

Accordingly, the current analysis focused on regional thalamic volumes collected longitudinally. The initial MRIs were taken from the work on FASD-related brain dysmorphology conducted at the University of Washington Fetal Alcohol and Drug Unit directed by Dr. Ann Streissguth. Dr. Fred Bookstein performed the initial brain imaging analyses (5) based on 3 groups matched on age and sex: the FAS, FAE, and control groups. The 20-year follow-up MRIs were acquired under the direction of Dr. Susan Stoner at the Addictions, Drug & Alcohol Institute at the University of Washington. The current objective was to parcellate the thalamus into 10 nuclei and further aggregate them into 4 regions to test the following 3 hypotheses: 1) cross-sectionally, at MRI1, both the FAS and FAE groups would have regional thalamic volume deficits relative to the control group, and the FAS volume deficits would be greater than those of the FAE group (i.e., control > FAE > FAS in regional volume); 2) longitudinally, MRI2 data would show volume declines in all 3 groups, with the same graded volume deficits observed as with MRI1; and 3) the volume deficits of the FAE and FAS groups would be suggestive of faster aging than in the control group regardless of sex.

METHODS AND MATERIALS

Details regarding participant study criteria, attrition, harmonization of longitudinal MRI data, and statistical analysis appear in the Supplement.

Participants

Two sets of MRI data separated by about 20 years are reported. The initial neuroimaging data (MRI1) were collected between 1997 and 2000, and the second set of data (MRI2) were collected between 2018 and 2021. The seminal studies on MRI1 were published by Bookstein *et al.* (4,5) with later cross-sectional analyses focused on subcortical structures (29) and the cerebellum (30). A 20-year follow-up study was conducted on about one-third of the original group who were willing and able to participate and whose data were of adequate quality for analysis (28).

Cross-Sectional Cohort. The entry diagnoses of the 179 participants with initial MRIs comprised 59 control individuals, 59 individuals with FAE, and 61 individuals with FAS. As described in our earlier publications (28,30), all participants were identified, recruited, clinically and neuropsychologically examined, and diagnosed with informed consent for MRI1 under the direction of Dr. Ann Streissguth through the FAS Follow-up Study at the University of Washington (4,5,31). Of the participants with FASD, systematic diagnosis (conducted mainly by Dr. David Smith or Dr. Sterling Clarren) used 1994 criteria to determine FAS and FAE. FAS required evidence of central nervous system dysfunction, growth deficit, and the presence of diagnostically defining facial features, whereas the classification of FAE was assigned when the full set of physical characteristics was not present in an individual with known heavy alcohol exposure prenatally (4).

Wechsler Adult Intelligence Scale-Revised IQs (32) comprised 3 measures: performance IQ (PIQ), verbal IQ (VIQ), and Full Scale IQ (FSIQ); the latter 2 were prorated over the available subtests. Prorated VIQs were available for all 179 participants; only 1 person in each of the FAE and FAS groups was missing PIQ and FSIQ scores (Table 1).

Both the initial MRI study and the current study were approved by the University of Washington Institutional Review Board. Consent was obtained according to the Declaration of Helsinki from adult participants, or their legal guardians when necessary, in which case assent was obtained from the participant. Numerous other reports based on the full or partial cohort have been published (4,29).

Longitudinal Cohort. Of the 179 participants with initial MRIs, attempts were made to contact 162 participants, excluding 12 participants with FASD who lived outside the United States. MRI2 data were acquired on average 21.6 years

Table 1. Demographic Data for the Three Groups

	Control		FAE		FAS		Control vs. FAE		Control vs. FAS		FAE vs. FAS	
	Mean (SD)	*n*	Mean (SD)	*n*	Mean (SD)	*n*	t/χ^2	*p*	*t*	*p*	*t*	*p*
Initial MRI												
Age, Years												
Female	19.49 (5.33)	30	20.25 (6.68)	29	20.15 (5.84)	31	−0.483	.6311	−0.454	.6515	0.067	.9472
Male	20.09 (5.63)	29	19.40 (5.21)	30	19.98 (5.64)	30	0.488	.6274	0.074	.9412	−0.414	.6804
Total	19.79 (5.44)	59	19.82 (5.94)	59	20.06 (5.70)	61	−0.031	.9754	−0.273	.7856	−0.031	.9754
Education, Years	11.71 (2.69)	59	10.21 (1.91)	58	9.84 (2.23)	57	3.484	.0007*	4.064	.0001*	0.942	.3482
WAIS												
VIQ prorated	108.27 (11.98)	59	82.68 (13.39)	59	79.74 (12.31)	61	10.941	.0001*	12.862	.0001*	1.253	.2128
PIQ	108.80 (15.44)	59	88.19 (16.26)	58	84.03 (15.29)	60	7.031	.0001*	8.790	.0001*	1.431	.1551
FSIQ prorated	109.37 (13.81)	59	83.38 (14.41)	58	79.92 (13.81)	60	9.963	.0001*	11.873	.0001*	1.360	.1768
Handedness, Right/Left		57/2		52/6		44/13	$\chi^2 = 10.544$	.0051*				
Ethnicity		59		59		61						
African American	–	9	–	5	–	2	$\chi^2 = 5.716$	.2214				
American Indian/Alaskan Native	–	13	–	17	–	18						
Caucasian	–	37	–	37		41						
Follow-Up MRI												
Age, Years												
Female	40.38 (6.19)	13	40.13 (5.77)	8	40.42 (4.87)	12	0.092	.9272	−0.018	.9859	−0.121	.9048
Male	43.38 (8.02)	13	44.82 (6.69)	11	41.17 (6.31)	12	−0.472	.6414	0.762	.4541	1.347	.1924
Total	41.88 (7.18)	26	42.84 (6.59)	19	40.79 (5.52)	24	−0.463	.6456	0.606	.5475	1.087	.2845
Education, Years	11.96 (2.71)	26	11.00 (1.89)	19	10.26 (2.09)	23	1.405	.1673	2.475	.0170	1.203	.2362
WAIS												
VIQ prorated	112.00 (10.60)	26	88.79 (11.19)	19	81.46 (11.31)	24	7.027	.0000*	9.832	.0000*	2.124	.0401
PIQ	113.12 (14.48)	26	94.26 (15.53)	19	86.13 (15.83)	24	4.137	.0002*	6.275	.0000*	−1.692	.0986
FSIQ prorated	113.81 (12.93)	26	90.47 (11.63)	19	81.92 (13.22)	24	6.338	.0000*	8.612	.0000*	2.255	.0296
Handedness, Right/Left	–	25/1	–	16/3	–	16/7	$\chi^2 = 6.366$	.0414				
Ethnicity												
African American	–	1	–	1	–	2	$\chi^2 = 1.458$	.8341				
American Indian/Alaskan Native	–	4	–	5	–	4						
Caucasian	–	21	–	13	–	18						

*Significant group effects with Bonferroni correction for 9 comparisons with $\alpha = 0.05$, $p \leq .006$.

FAE, fetal alcohol exposure; FAS, fetal alcohol syndrome; FSIQ, Full Scale IQ; MRI, magnetic resonance imaging; PIQ, performance IQ; VIQ, verbal IQ; WAIS, Wechsler Adult Intelligence Scale.

following MRI1 for the control, 21.8 years for the FAE, and 20.8 years for the FAS groups. Initial IQ scores were available for all 69 participants in the follow-up cohort. FASD-specific head and facial morphometric feature scores, determined by dysmorphologists at the follow-up examination and used for categorizing FAS (33), were available for all 69 participants in the longitudinal analysis from the CIFASD4 (Collaborative Initiative on Fetal Alcohol Spectrum Disorders) dysmorphology database (https://cifasd.org/data-sharing/). Continuous and one categorical metrics available enabling parametric testing of correlations with MRI brain volumes were occipitofrontal circumference, inner canthal distance, maxillary arch, mandibular arch, left and right palpebral fissure length, philtrum length, and vermillion border lipometer [cf. (34)].

MRI Acquisition and Processing

As described (28), native T1-weighted MRI legacy data at the first scan were acquired on a 1.5T GE Signa system (sagittal spoiled gradient recalled, TR = 29 ms, TE = 8 ms, flip angle = 45°, FOV = 220 mm, thickness = 1.5 mm, slices = 124, matrix = 256 × 256) (4). The follow-up MRIs were acquired on a Philips Ingenia Medical System 3T scanner (sagittal GR MP [gradient recalled with magnetization preparation], TR = 6.37 ms, TE = 2.93 ms, ETL [echo train length] = 150, FOV = 240 mm, thickness = 1.0 mm, matrix = 256 × 256) at the University of Washington and preserved as NIfTI files for processing.

MRI processing for regional brain measures and ICV was performed by the longitudinal software pipeline SIBIS (27). The thalamus was parcellated as described previously (19,20,35). The THalamus Optimized Multi-Atlas Segmentation is a multi-atlas segmentation method (17) that produced separate unilateral estimates of total bilateral thalamic volume and 10 bilateral nuclei (20 left/right, unilateral volumes), which were then aggregated into 4 functionally relevant regions: anterior = anterior ventral nucleus (AV); ventral = ventral lateral anterior (VLa) + ventral lateral posterior (VLp) + ventral anterior (VA) + ventral posterior lateral (VPl); posterior = pulvinar (Pul) + lateral geniculate nucleus (LGN) + medial geniculate nucleus (MGN); and medial = centromedian (CM) + mediodorsal (MD). Parcellation, whether for regions or nuclei, included about 70% of the total thalamic volume. Because thalamic volume is highly correlated with brain size, all thalamic measures were expressed as native values and as a percentage of one's own ICV (%ICV).

Statistical Analysis

Following the procedures of our earlier longitudinal investigation (28), statistical analysis was performed using R version 3.5.1 (36) on bilateral thalamic volumes, first using regional volumes and then nucleus volumes. The primary statistic for comparisons at initial study for all participants and for between returners and nonreturners was a general linear model (*lm*), which separately predicted the volume of each region as a function of diagnostic group (control, FAE, FAS) + sex + age. Next, *lm*s analyzed cross-sectional comparisons of the regional and nuclear volumes of the 3 returning groups. The longitudinal analysis used a linear mixed-effects model (*lmer*), which included age (as a surrogate for MRI1 vs. MRI2) as the repeated measure. Interactions with age tested potential group differences in rates of change from the original to the follow-up scan. The model outputs produced *t* and *p* significance values for each diagnostic group relative to the control group. To compare the FAE group and the FAS group, the model was rerun with FAE as the index level. Paired *t* tests were used to test for potential differences in thalamic volumes within each group.

RESULTS

Cross-Sectional Comparisons

At MRI1, the *lm* analyses across the groups controlling for age and sex revealed a stepwise volume deficit in ICV wherein the FAE group had smaller volumes than the control group, and the FAS group had smaller volumes than the FAE group (Figure 1; Tables 2 and 3). Although the age factor was not significant, the sex factor was significant, reflecting the known somatic size difference related to sex.

Regional Thalamic Volumes. The *lm* analyses comparing the 4 native regional volumes and total thalamus while controlling for age and sex indicated that volumes were significantly smaller in the FAE and FAS groups than in the control group ($p < .001$ per region with familywise Bonferroni correction) (Table 2 and Figure 2). Similar analyses conducted to compare the FAE and FAS groups indicated that the FAS ventral region was significantly smaller than that of the FAE group (Table 3 and Figure 2), and the total and anterior regions showed trends for the FAS group to have smaller volumes than the FAE group. For most comparisons, sex was a significant factor, and age was a less important factor.

The same set of comparisons were made using *lm* models based on volumes corrected for ICV by expressing the volume of each thalamic measure as %ICV. Relative to the control group, the smaller volumes of the FAE and FAS

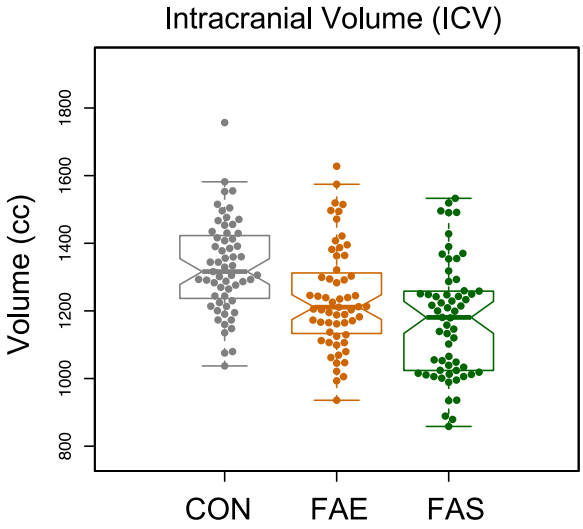

Figure 1. Bee swarm boxplots of ICV (cc) of control (CON) (gray), fetal alcohol exposure (FAE) (orange), and fetal alcohol syndrome (FAS) (green) participants.

Table 2. Group Volume Differences at Magnetic Resonance Imaging 1

	Control	FAE	FAS	Control vs. FAE		Control vs. FAS		Age		Sex		
	Mean (SD)	Mean (SD)	Mean (SD)	*t*	*p*	*t*	*p*	*t*	*p*	*t*	*p*	Adjusted R^2
ICV	1330.476 (137.639)	1236.703 (152.750)	1171.862 (169.658)	−3.852	.0002*	−6.378	.0000*	−1.605	.1103	7.121	.0000*	0.3384
Controlling for Age and Sex but Not ICV												
Native Volumes												
Regions[a]												
Anterior	0.248 (0.045)	0.204 (0.062)	0.176 (0.064)	−4.149	.0001*	−6.860	.0000*	0.340	.7344	0.980	.3282	0.2006
Ventral	3.217 (0.327)	2.875 (0.443)	2.642 (0.521)	−4.448	.0000*	−7.429	.0000*	−1.106	.2702	3.803	.0002*	0.2761
Posterior	3.290 (0.334)	2.981 (0.405)	2.816 (0.567)	−4.020	.0001*	−6.097	.0000*	−3.314	.0011	3.652	.0003*	0.2509
Medial	1.523 (0.127)	1.416 (0.182)	1.376 (0.228)	−3.352	.0010*	−4.531	.0000*	−2.341	.0203	3.749	.0002*	0.1761
Total	11.996 (1.085)	10.935 (1.404)	10.309 (1.775)	−4.279	.0000*	−6.721	.0000*	−2.685	.0079	4.286	.0000*	0.2783
Nuclei[b]												
AV	0.248 (0.045)	0.204 (0.062)	0.176 (0.064)	−4.149	.0001*	−6.860	.0000*	0.340	.7344	0.980	.3282	0.2006
VA	0.642 (0.078)	0.568 (0.113)	0.520 (0.121)	−3.939	.0001*	−6.418	.0000*	−1.336	.1834	2.927	.0039*	0.2144
VLa	0.167 (0.018)	0.154 (0.024)	0.141 (0.027)	−3.129	.0021*	−6.226	.0000*	−0.410	.6825	3.734	.0003*	0.2159
VLp	1.784 (0.19)	1.593 (0.256)	1.472 (0.300)	−4.280	.0000*	−6.963	.0000*	−0.592	.5547	3.739	.0003*	0.2513
VPL	0.624 (0.074)	0.560 (0.085)	0.509 (0.110)	−4.029	.0001*	−7.176	.0000*	−1.997	.0474	3.470	.0007*	0.2658
Pul	2.927 (0.299)	2.666 (0.371)	2.523 (0.505)	−3.794	.0002*	−5.780	.0000*	−3.467	.0007*	3.560	.0005*	0.2396
LGN	0.225 (0.044)	0.186 (0.033)	0.168 (0.052)	−4.926	.0000*	−7.226	.0000*	−1.248	.2138	2.273	.0243	0.2440
MGN	0.137 (0.016)	0.129 (0.018)	0.125 (0.029)	−2.178	.0307	−3.333	.0010*	−1.476	.1418	4.534	.0000*	0.1461
CM	0.211 (0.024)	0.200 (0.036)	0.182 (0.040)	−1.962	.0513	−4.783	.0000*	−1.062	.2898	3.050	.0026*	0.1440
MD	1.311 (0.116)	1.216 (0.155)	1.193 (0.196)	−3.447	.0007*	−4.194	.0000*	−2.475	.0143	3.668	.0003*	0.1681
Controlling for Age and Sex as a Percent of ICV												
Regions[a]												
Anterior %	0.019% (0.003%)	0.017% (0.005%)	0.015% (0.005%)	−2.697	.0077*	−4.740	.0000*	1.037	.3011	−1.947	.0531	0.1160
Ventral %	0.242% (0.016%)	0.232% (0.023%)	0.225% (0.026%)	−2.426	.0163	−4.334	.0000*	0.365	.7158	−2.366	.0191	0.1037
Posterior %	0.249% (0.025%)	0.242% (0.028%)	0.241% (0.038%)	−1.101	.2724	−1.273	.2045	−2.331	.0209	−2.102	.0370	0.0418
Medial %	0.115% (0.009%)	0.115% (0.013%)	0.118% (0.015%)	0.059	.9534	1.320	.1885	−1.059	.2911	−3.018	.0029*	0.0450
Total %	0.905% (0.060%)	0.886% (0.077%)	0.880% (0.089%)	−1.303	.1942	−1.768	.0789	−1.774	.0779	−3.004	.0031*	0.0609
Nuclei[b]												
AV %	0.019% (0.003%)	0.017% (0.005%)	0.015% (0.005%)	−2.697	.0077	−4.740	.0000*	1.037	.3011	−1.947	.0531	0.1160
VA %	0.048% (0.004%)	0.046% (0.006%)	0.044% (0.007%)	−2.470	.0145	−4.047	.0001*	−0.493	.6223	−1.968	.0506	0.0864
VLa %	0.013% (0.001%)	0.012% (0.001%)	0.012% (0.001%)	−0.490	.6250	−2.550	.0116	1.494	.1369	−2.179	.0307	0.0541
VLp %	0.134% (0.011%)	0.129% (0.015%)	0.125% (0.016%)	−2.176	.0309	−3.670	.0003*	0.979	.3288	−1.973	.0501	0.0749
VPL %	0.047% (0.005%)	0.045% (0.005%)	0.044% (0.007%)	−1.604	.1105	−3.397	.0008*	−0.778	.4377	−2.001	.0470	0.0643
Pul %	0.221% (0.021%)	0.217% (0.027%)	0.216% (0.034%)	−0.854	.3941	−0.929	.3542	−2.499	.0134**	−2.181	.0305	0.0432
LGN %	0.017% (0.004%)	0.015% (0.002%)	0.014% (0.004%)	−3.202	.0016*	−4.473	.0000*	−0.576	.5655	−1.096	.2746	0.0959
MGN %	0.010% (0.001%)	0.011% (0.001%)	0.011% (0.002%)	0.432	.6662	1.157	.2490	−0.442	.6588	−0.432	.6660	−0.0129
CM %	0.016% (0.002%)	0.016% (0.002%)	0.016% (0.003%)	0.458	.6475	−0.940	.3487	−0.096	.9237	−1.757	.0807	0.0061
MD %	0.099% (0.008%)	0.099% (0.011%)	0.102% (0.013%)	−0.033	.9735	1.702	.0905	−1.181	.2394	−3.042	.0027*	0.0558

*Indicates $p \leq .05$ corrected p value.

AV, anterior ventral nucleus; CM, centromedian; FAE, fetal alcohol exposure; FAS, fetal alcohol syndrome; ICV, intracranial volume; LGN, lateral geniculate nucleus; MD, mediodorsal; MGN, medial geniculate nucleus; Pul, pulvinar; VA, ventral anterior; VLa, ventral lateral anterior; VLp, ventral lateral posterior; VPL, ventral posterior lateral.

[a]Familywise Bonferroni correction for 4 comparisons with $\alpha = 0.05$, $p \leq .0125$.

[b]Familywise Bonferroni correction for 10 comparisons with $\alpha = 0.05$, $p \leq .005$.

Table 3. FAE vs. FAS Group Volume Differences Controlling for Age and Sex

	FAE vs. FAS		Age		Sex	
	t	*p*	*t*	*p*	*t*	*p*
ICV	−2.365	.0197*	−1.717	.0887	5.697	.0000*
Native Volumes						
Regions[a]						
Anterior	−2.450	.0158	0.378	.7065	0.419	.6763
Ventral	−2.633	.0096*	−1.209	.2293	2.568	.0115*
Posterior	−1.852	.0665	−3.083	.0026*	3.073	.0026*
Medial	−1.014	.3129	−2.073	.0404	2.763	.0067*
Total	−2.160	.0328	−2.513	.0133	3.089	.0025*
Nuclei[b]						
AV	−2.450	.0158	0.378	.7065	0.419	.6763
VA	−2.188	.0307	−1.319	.1897	1.741	.0844
VLa	−2.755	.0068	−0.280	.7803	2.600	.0105
VLp	−2.371	.0194	−0.853	.3954	2.624	.0099
VPL	−2.861	.0050*	−1.867	.0644	2.403	.0179
Pul	−1.767	.0799	−3.237	.0016*	2.808	.0059
LGN	−2.318	.0222	−1.044	.2986	3.584	.0005*
MGN	−1.025	.3074	−1.463	.1463	4.485	.0000*
CM	−2.514	.0133	−0.889	.3759	2.826	.0055
MD	−0.637	.5256	−2.226	.0280	2.609	.0103
ICV-Corrected Volumes						
Regions[a]						
Anterior %	−1.830	.0699	1.108	.2702	−1.727	.0868
Ventral %	−1.717	.0886	0.235	.8143	−2.199	.0298
Posterior %	−0.139	.8895	−2.089	.0389	−1.344	.1814
Medial %	1.122	.2642	−0.807	.4212	−2.314	.0224
Total %	−0.418	.6770	−1.577	.1175	−2.581	.0111*
Nuclei[b]						
AV %	−1.830	.0699	1.108	.2702	−1.727	.0868
VA %	−1.408	.1619	−0.463	.6445	−2.073	.0404
VLa %	−1.887	.0617	1.717	.0886	−1.958	.0526
VLp %	−1.345	.1813	0.672	.5028	−1.727	.0868
VPL %	−1.645	.1027	−0.615	.5395	−1.918	.0576
Pul %	−0.053	.9575	−2.252	.0262	−1.595	.1135
LGN %	−1.296	.1976	−0.279	.7806	0.731	.4663
MGN %	0.676	.5001	−0.423	.6733	0.631	.5292
CM %	−1.283	.2022	0.095	.9249	−0.803	.4238
MD %	1.550	.1239	−0.940	.3494	−2.466	.0151

ICV-corrected volumes are expressed as % of ICV.

*Indicates $p \leq .05$ corrected *p* value.

AV, anterior ventral nucleus; CM, centromedian; FAE, fetal alcohol exposure; FAS, fetal alcohol syndrome; ICV, intracranial volume; LGN, lateral geniculate nucleus; MD, mediodorsal; MGN, medial geniculate nucleus; Pul, pulvinar; VA, ventral anterior; VLa, ventral lateral anterior; VLp, ventral lateral posterior; VPL, ventral posterior lateral.

[a]Familywise Bonferroni correction for 4 comparisons with $\alpha = 0.05$, $p \leq .0125$.

[b]Familywise Bonferroni correction for 10 comparisons with $\alpha = 0.05$, $p \leq .005$.

groups persisted following %ICV correction in the anterior region (Table 2 and Figure 2). The FAS volume also persisted in the ventral region, with a trend in the FAE comparison with the control group. In contrast to the results based on the native volumes, the %ICV correct volumes fully attenuated regional differences between the FAE and FAS groups (Table 3 and Figure 2).

Nuclear Thalamic Volumes. The *lm* analyses comparing the 10 nuclear volumes, while controlling for age and sex, across the 3 groups indicated significant deficits in 8 nuclei of the FAE and in all 10 nuclei of the FAS ($p < .001$ per region with familywise Bonferroni correction) groups (Table 2 and Figure 3); deficit trends that were evident in the 2 nuclear volumes of the FAE group did not meet multiple

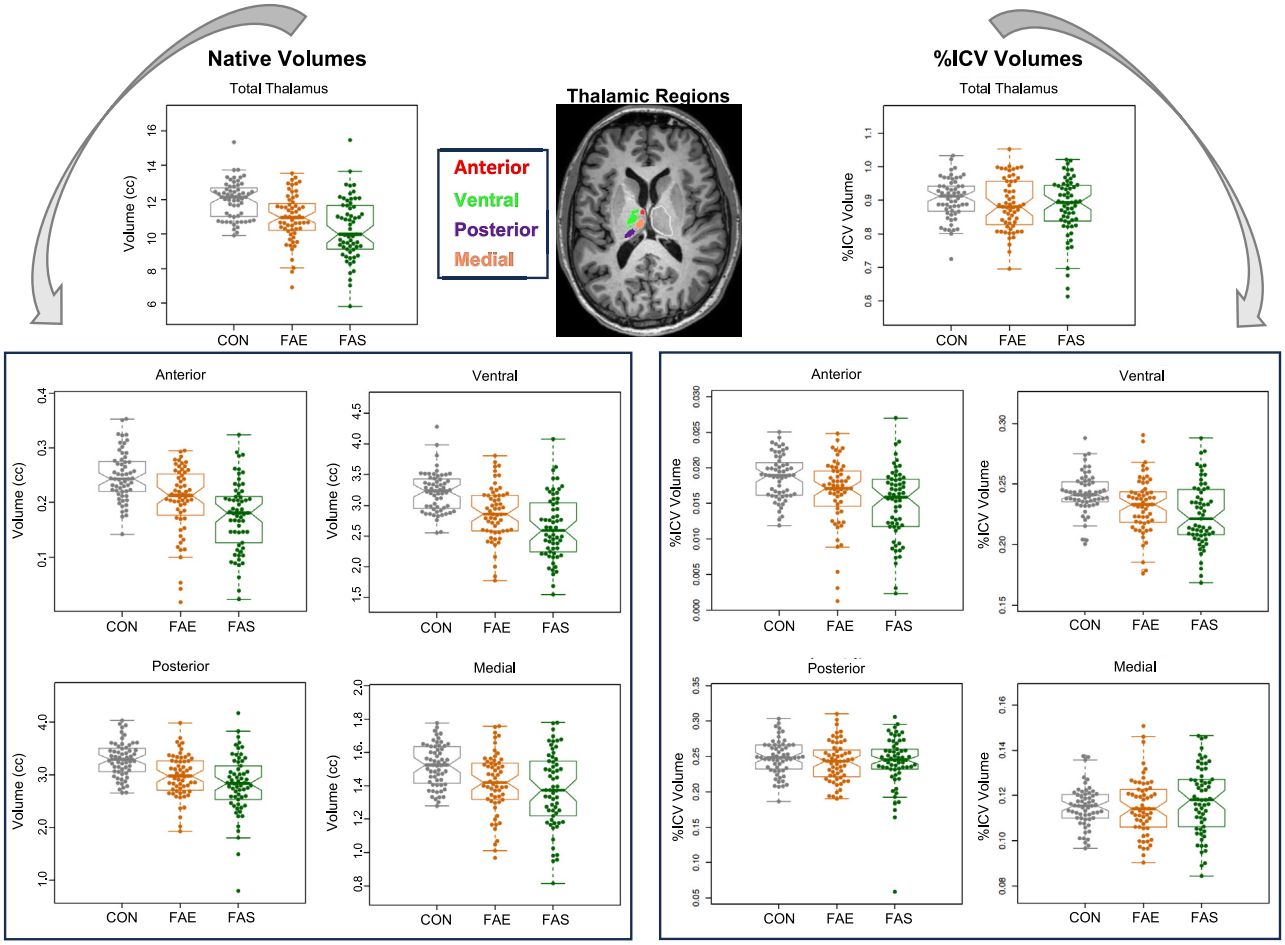

Figure 2. Five bee swarm boxplots on the left display native volumes of thalamic regions and total thalamus. Five bee swarm boxplots on the right display percentage intracranial volume (%ICV)–adjusted volumes of thalamic regions and the total thalamus. Each dot represents a participant: control (CON) (gray), fetal alcohol exposure (FAE) (orange), and fetal alcohol syndrome (FAS) (green). The 4 thalamic regions are color coded and displayed on an axial magnetic resonance imaging slice of a control participant.

comparison correction. Comparisons of volumes of the FAE and FAS groups revealed smaller volumes in the FAS than the FAE group that met Bonferroni correction in the VPL, with statistical trends evident in 6 of the 9 remaining volumes (Table 2).

With ICV correction and relative to the control group, the FAE group had a significant volume deficit in the LGN, with trends in the AV, VA, and VLp. The FAS group had significant volume deficits in the AV, VA, VLp, VPL, and LGN, with a trend in the VLa. The ICV correction removed all FAE versus FAS group differences in nuclear volumes (Table 3 and Figure 3).

Relationships Between IQ Scores and Thalamic Regional Volumes. Combining the FAE and FAS groups yielded positive correlations between PIQ scores and thalamic regional volumes, although only the medial volume met significance following correction for multiple comparisons (Figure 4). Correlations based on VIQ and FSIQ scores were not significant (Table 4).

Longitudinal Assessment of Volumetric Changes by Group

The 20-year follow-up analysis included 26 control participants, 19 participants with FAE, and 24 participants with FAS (bottom half of Table 1). Comparing demographic data of returners and nonreturners at MRI1 revealed that the ages of the returning and nonreturning groups were about the same (Table 5). In general, the returners had more education and higher IQ scores than the nonreturners in all groups, although these differences were only significant (following correction for multiple comparisons) for the FAE group.

Regional Thalamic Volumes. Despite a trend for smaller ICV across all groups, within-group paired *t* tests revealed no

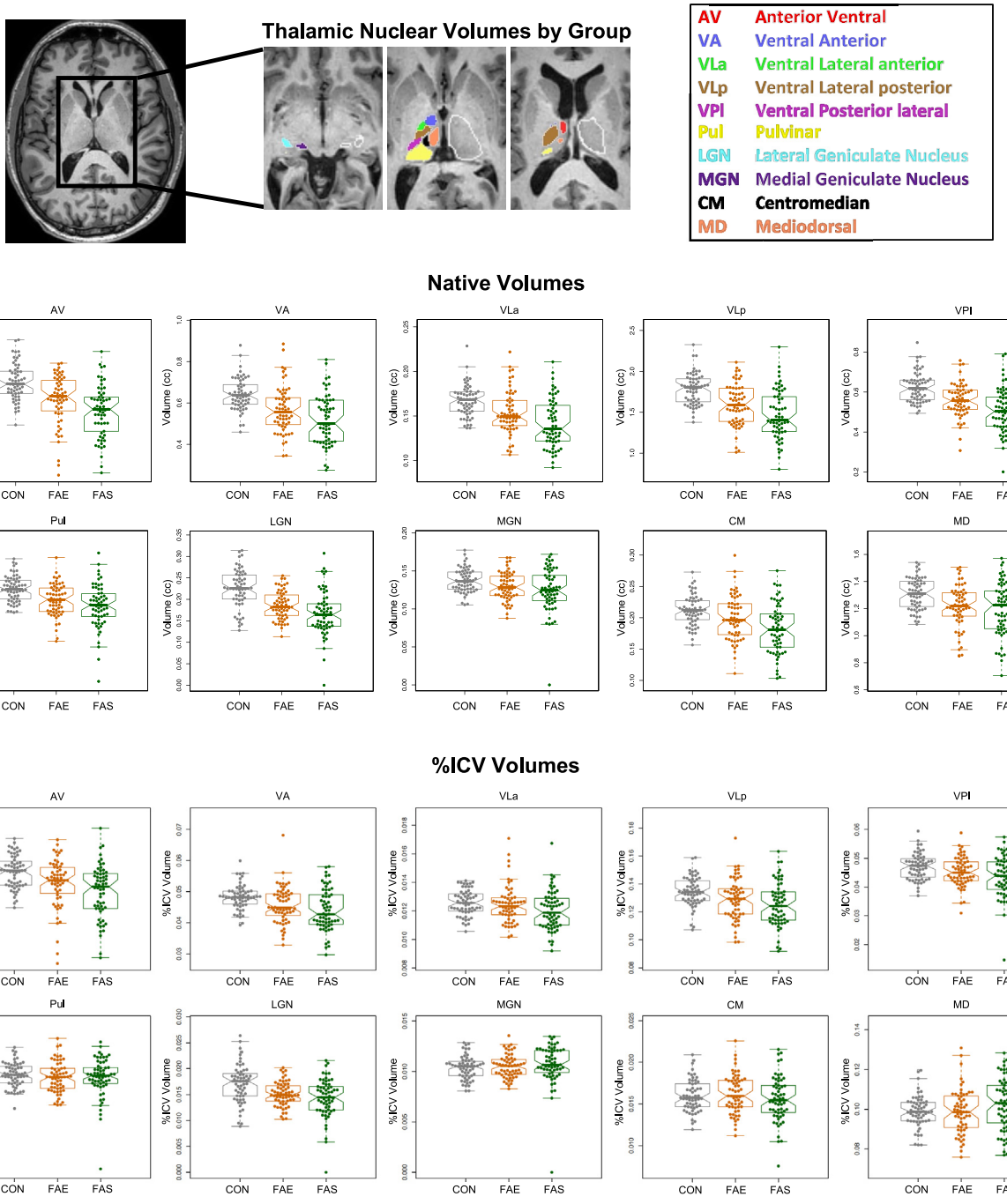

Figure 3. Axial magnetic resonance images from T1-weighted data (top) of a control man [modified with permission from Pfefferbaum *et al.* (19)]. The cutouts are from 3 different axial levels of volumes used in the analysis process. From radiological orientation, the white outline in the right hemispheres (left side of the cutout images) encompasses the total thalamus on that slice; the color coding on the left hemispheres (right side of the cutout images) indicates the 10 thalamic nuclei. (Top) Bee swarm boxplots of native volumes of thalamic regions. (Bottom) Bee swarm boxplots of percentage intracranial volume (%ICV)–adjusted volumes per group. Each dot represents a participant: control (CON) (gray), fetal alcohol exposure (FAE) (orange), and fetal alcohol syndrome (FAS) (green).

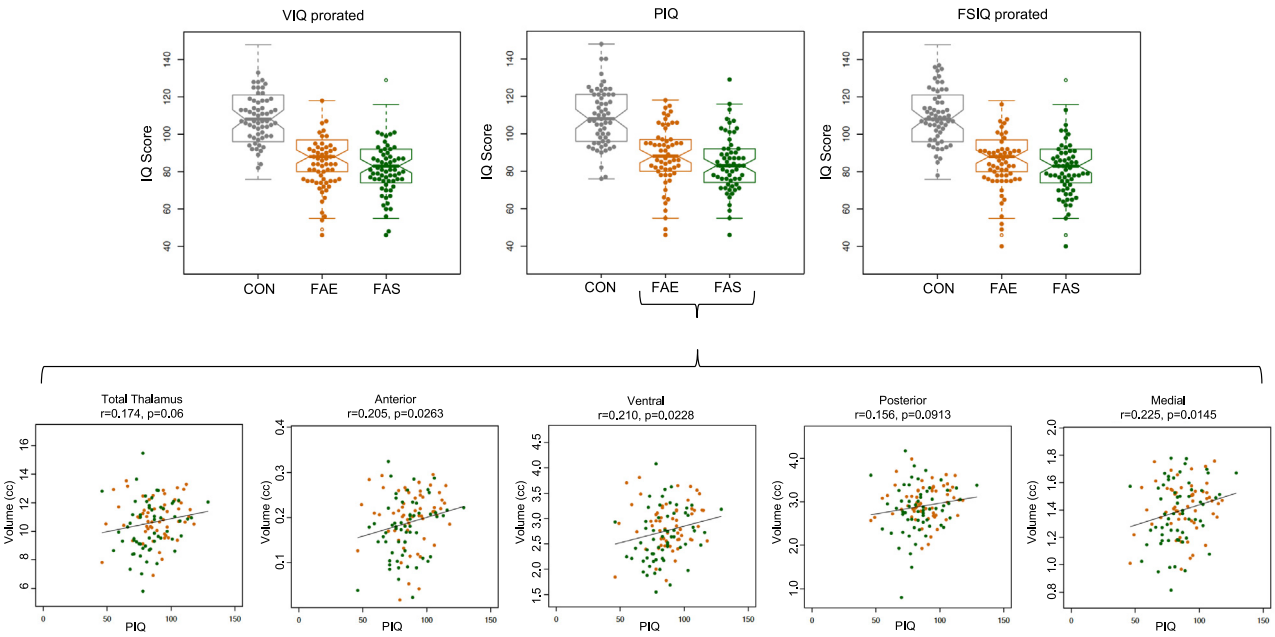

Figure 4. (Top) Bee swarm boxplots of verbal IQ (VIQ) (prorated), performance IQ (PIQ), and Full Scale IQ (FSIQ) (prorated) scores of each participant in each group. (Bottom) Correlations between the PIQ scores of the combined fetal alcohol exposure (FAE) and fetal alcohol syndrome (FAS) groups and raw regional thalamic volumes. CON, control.

Table 4. IQ Measures Correlated With Raw Thalamic Volumes of the Combined FAE+FAS Groups Controlling for Age and Sex

	t→Correlation		Age		Sex	
	t	*p*	*t*	*p*	*t*	*p*
PIQ						
Region[a]						
Anterior	2.166	.0324*	1.741	.0844	0.795	.4282
Ventral	2.396	.0182*	2.059	.0418*	0.345	.7306
Posterior	2.137	.0347*	2.327	.0217*	0.298	.7660
Medial	2.786	.0063*	2.335	.0213*	0.210	.8343
Total	2.217	.0286*	2.258	.0258*	0.282	.7787
Nuclei[b]						
AV	2.166	.0324*	1.741	.0844	0.795	.4282
VA	2.087	.0391*	2.040	.0436*	0.561	.5762
VLa	0.743	.4591	1.798	.0749	0.707	.4808
VLP	2.377	.0191*	1.983	.0497*	0.331	.7413
VPL	2.361	.0199*	2.178	.0314*	0.410	.6829
Pul	2.041	.0436*	2.317	.0223*	0.376	.7077
LGN	2.487	.0143*	2.059	.0418*	0.050	.9605
MGN	1.527	.1296	1.984	.0497*	0.252	.8016
CM	2.176	.0316*	1.995	.0485*	0.322	.7479
MD	2.769	.0066*	2.362	.0199*	0.257	.7973
VIQ Prorated						
Region[a]						
Anterior	1.082	.2815	−0.018	.9857	−0.184	.8539
Ventral	1.390	.1670	0.171	.8642	−0.455	.6498
Posterior	0.691	.4907	0.203	.8392	−0.323	.7473
Medial	1.207	.2297	0.243	.8082	−0.436	.6636
Total	0.830	.4080	0.202	.8403	−0.361	.7185

Table 4. Continued

	t→Correlation		Age		Sex	
	t	*p*	*t*	*p*	*t*	*p*
Nuclei[b]						
AV	1.082	.2815	−0.018	.9857	−0.184	.8539
VA	1.405	.1626	0.187	.8519	−0.363	.7175
VLa	0.368	.7134	0.025	.9800	−0.221	.8257
VLP	1.535	.1275	0.139	.8895	−0.497	.6202
VPL	0.726	.4690	0.138	.8908	−0.292	.7707
Pul	0.619	.5371	0.191	.8486	−0.291	.7719
LGN	1.180	.2405	0.130	.8965	−0.501	.6170
MGN	0.549	.5843	0.088	.9297	−0.339	.7349
CM	0.888	.3766	0.089	.9291	−0.358	.7211
MD	1.214	.2271	0.261	.7949	−0.423	.6734
FSIQ Prorated						
Region[a]						
Anterior	1.753	.0822	0.786	.4333	0.451	.6530
Ventral	2.159	.0329	1.069	.2873	0.042	.9669
Posterior	1.641	.1036	1.260	.2103	0.079	.9368
Medial	2.329	.0216	1.283	.2023	−0.040	.9685
Total	1.785	.0769	1.217	.2260	0.044	.9646
Nuclei[b]						
AV	1.753	.0822	0.786	.4333	0.451	.6530
VA	1.935	.0554	1.066	.2887	0.226	.8219
VLa	0.671	.5034	0.850	.3970	0.375	.7082
VLP	2.239	.0271	1.008	.3158	0.007	.9943
VPL	1.794	.0754	1.124	.2632	0.165	.8695
Pul	1.580	.1170	1.259	.2105	0.136	.8923
LGN	1.801	.0744	1.017	.3115	−0.076	.9395
MGN	1.159	.2488	0.986	.3262	0.058	.9539
CM	1.718	.0885	0.989	.3247	0.085	.9323
MD	2.340	.0210	1.313	.1919	−0.006	.9953

*Indicates $p \leq .05$ corrected p value.

AV, anterior ventral nucleus; CM, centromedian; FAE, fetal alcohol exposure; FAS, fetal alcohol syndrome; FSIQ, Full Scale IQ; LGN, lateral geniculate nucleus; MD, mediodorsal; MGN, medial geniculate nucleus; PIQ, performance IQ; Pul, pulvinar; VA, ventral anterior; VIQ, verbal IQ; VLa, ventral lateral anterior; VLp, ventral lateral posterior; VPL, ventral posterior lateral.

[a]Familywise Bonferroni correction for 4 comparisons with $\alpha = 0.05$, $p \leq .0125$.

[b]Familywise Bonferroni correction for 10 comparisons with $\alpha = 0.05$, $p \leq .005$.

significant changes. Overall, the stepwise volume differences persisted over time: control > FAE > FAS (Figure 5 and Table 6). Within the 3 groups, the ventral, posterior, and total regions were significantly smaller at MRI2 than at MRI1; the anterior region was not significantly different, and the medial region was larger for the control participants (Table 6; Figure 6, left pair).

Based on native volumes, *lmer* analyses were used to compare each affected group against the control group. The model compared region as a function of diagnosis + age + sex + age × diagnosis and was applied in analyses involving the regional and nuclear, native, and the %ICV volumes. The diagnosis × age interactions tested whether the groups differed in change from MRI1 to MRI2. The only interaction observed was for the medial volume, which declined faster in the FAE group than in the control group (Table 7). The *lmer* analyses, in which age-volume change interactions for FAS compared with FAE were tested for, failed to identify any regional interactions (Table 7).

Following the same set of analyses used with native volumes, analyses based on regional volumes adjusted for %ICV yielded the same pattern of within-group MRI1 to MRI2 declines observed with native volumes (Table 6 and Figure 5).

The *lmer* analyses with %ICV-corrected volumes revealed that brain-size correction attenuated all group differences, showing only a trend for the medial volume to be proportionately smaller in the FAE than control group (Table 7 and Figure 6). None of the age × diagnosis interactions were significant for the FAE-FAS group comparison (Table 7 and Figure 6).

Nuclear Thalamic Volumes. Paired *t* tests for native nuclear volumes revealed declines in the VA, VLp, and Pul in each of the 3 groups that were significant in 5 comparisons

Table 5. Demographic Data at Initial Examination for Returner vs. Nonreturner by Diagnostic Group

	Control						FAE						FAS					
	Returner		Nonreturner				Returner		Nonreturner				Returner		Nonreturner			
	Mean	*n*, F/M	Mean	*n*, F/M	t/χ^2	*p*	Mean	*n*, F/M	Mean	*n*, F/M	t/χ^2	*p*	Mean	*n*, F/M	Mean	*n*, F/M	t/χ^2	*p*
Age, Years	20.2	13/13	19.5	17/16	0.503	.6173	21.0	8/11	19.3	21/19	1.017	.3165	19.7	12/12	20.3	19/18	−0.368	.7143
Education, Years	12.0	13/13	11.5	17/16	0.629	.5319	11.0	8/11	9.8	21/18	2.262	.0301*	10.3	11/12	9.6	17/17	1.190	.2394
WAIS																		
VIQ prorated	112.0	13/13	105.3	17/16	2.231	.0297*	88.8	8/11	79.8	21/19	2.701	.0099*	81.5	12/12	78.6	19/18	0.903	.3703
PIQ	113.1	13/13	105.4	17/16	1.969	.0539	94.3	8/11	85.2	20/19	2.060	.0466*	86.1	12/12	82.6	18/18	0.854	.3975
FSIQ prorated	113.8	13/13	105.9	17/16	2.282	.0264*	90.5	8/11	79.9	20/19	2.984	.0046**	81.9	12/12	78.6	18/18	0.955	.3444
Handedness, Right/Left	–	25/1	–	32/1	$\chi^2 = 0.030$	.8635	–	16/3	–	36/3	$\chi^2 = 0.090$	.3419	–	16/7	–	28/6	$\chi^2 = 1.274$	.2590
Ethnicity																		
African American	–	1	–	8	$\chi^2 = 7.316$	.0258*	–	1	–	4	$\chi^2 = 0.547$	.7606	–	2	–	0	$\chi^2 = 3.517$	.1723
American Indian/Alaskan Native	–	4	–	9			–	5	–	12			–	4	–	14		
Caucasian	–	21	–	16			–	13	–	24			–	18	–	23		

In all cases, returners > nonreturners either numerically or significantly.
*Indicates $p \leq .05$ corrected *p* value.
F, female; FAE, fetal alcohol exposure; FAS, fetal alcohol syndrome; FSIQ, Full Scale IQ; M, male; PIQ, performance IQ; VIQ, verbal IQ; WAIS, Wechsler Adult Intelligence Scale.

(Table 6), while maintaining the stepwise diagnostic effect: control > FAE > FAS. Volume declines were small and not significant in the VPL, LGN, or MGN in all groups. Volumes were insignificantly larger at MRI2 than at MRI1 in the AV (except for FAS), VLa, and CM and larger for MD in the control group only (Figure 7).

The *lmer* analyses using native nuclear volumes revealed only one trend, which suggested a greater decline in MD of the FAE group relative to the control group. This trend was also observed for %ICV-corrected volumes. No other age × diagnosis interaction was significant for any group comparison (Table 7 and Figure 8).

Dysmorphology Measures and Relationships With Thalamic Regional Volumes. Head and orofacial morphology scores were acquired at MRI2. Given that a diagnosis of FAS was dependent on facial dysmorphic observations, we expected that the degree of dysmorphology would be greater in the FAS group than in either the FAE or the control group. Although the FAS group generally had scores in the direction of greater dysmorphology on most measures (Figure 9), *lm* tests revealed significant group differences between the control and the FAS (but not the FAE) group on 4 measures: occipitofrontal circumference ($t = -2.900$, $p = .0053$), palpebral fissure length (left: $t = -4.212$, $p = .00009$; right: $t = -4.217$, $p = .00009$), and vermillion border lipometer ($t = 4.162$, $p = .0001$).

Correlations with MRI volumes indicated that the occipitofrontal circumference measure correlated, although imperfectly, with the MRI-derived ICV in the control group ($r = 0.452$, $p = .0232$) and the FAS group ($r = 0.788$, $p = .0001$) but not the FAE group ($r = 0.344$, $p = .2290$). None of the remaining continuous morphometric measures (philtrum, palpebral fissure length, or vermillion border) were correlated in the expected direction with thalamic volume or ICV.

DISCUSSION

The test outcomes supported the first 2 hypotheses but not the third. Specifically, we found that cross-sectionally, at MRI1, both the FAS and FAE groups had regional thalamic volume deficits relative to the control group, and the FAS volume deficits were greater than those of the FAE group. Longitudinally, MRI2 data showed volume declines in some regions and nuclei of all 3 groups while maintaining the same graded volume deficits observed at MRI1. By contrast, none of the volume deficits in either the FAE or FAS groups indicated faster aging than that observed in the control group, with the possible exception of the medial region in the FAE group.

The native volumes of every thalamic region and nucleus were smaller, either significantly or at trend levels, in the FAE and FAS groups than in the control group. Furthermore, in all but the anterior region, the volumes of the FAS group were smaller than those of the FAE group. Adjusting the thalamic volumes for differences in somatic size by using % ICV scores yielded an enduring stepwise pattern of group volume differences: control > FAE > FAS. Although the

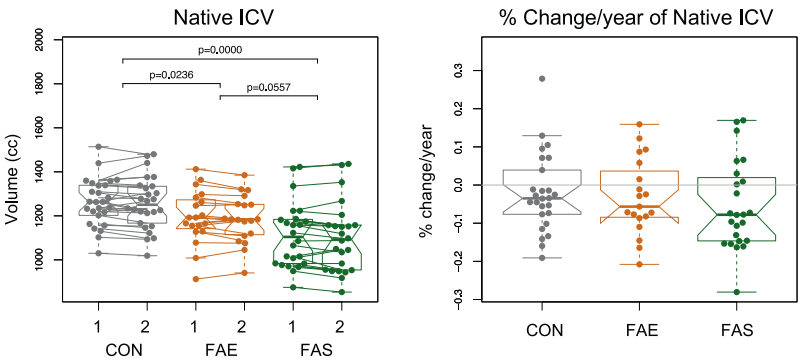

Figure 5. (Left) Bee swarm boxplots on the left are native intracranial volume (ICV) at magnetic resonance imaging (MRI) 1 and MRI2. The brackets at the top with *p* values indicate statistical results of group differences. (Right) The same data with ICV expressed as percentage change over the 20-year interval. CON, control; FAE, fetal alcohol exposure; FAS, fetal alcohol syndrome.

Table 6. Longitudinal Group Comparison of Thalamic Volumes: Paired *t* Tests

	MRI1 vs. MRI2 Paired *t* Test					
	CON		FAE		FAS	
	t	*p*	*t*	*p*	*t*	*p*
ICV	−0.798	.4326	−1.527	.1442	−2.014	.0559
Regions[a]						
Anterior	1.384	.1786	0.610	.5494	−0.638	.5300
Ventral	−3.074	.0050*	−2.584	.0187	−4.187	.0004*
Posterior	−5.999	.0000*	−4.853	.0001*	−5.179	.0000*
Medial	2.714	.0119*	−1.796	.0893	−0.209	.8360
Total	−8.641	.0000*	−6.116	.0000*	−7.992	.0000*
Nuclei[b]						
AV	1.384	.1786	0.610	.5494	−0.638	.5300
VA	−5.170	.0000*	−2.397	.0276	−3.867	.0008*
VLa	5.459	.0000*	2.544	.0204	6.601	.0000*
VLp	−2.802	.0097	−2.852	.0106	−4.463	.0002*
VPL	−1.157	.2581	−1.275	.2186	−1.178	.2508
Pul	−5.953	.0000*	−4.832	.0001*	−5.072	.0000*
LGN	−2.050	.0510	−1.754	.0965	−2.598	.0161
MGN	−2.491	.0197	−3.074	.0065	−0.708	.4859
CM	2.974	.0064	0.273	.7876	2.277	.0324
MD	1.944	.0633	−2.117	.0485	−0.675	.5065
%ICV-Corrected Volumes						
Regions[a]						
Anterior %	1.423	.1671	0.668	.5126	−0.364	.7190
Ventral %	−2.815	.0094*	−2.188	.0421	−3.111	.0049*
Posterior %	−5.451	.0000*	−3.924	.0010*	−4.094	.0004*
Medial %	3.877	.0007*	−1.238	.2317	0.710	.4847
Total %	−8.992	.0000*	−6.034	.0000*	−7.550	.0000*
Nuclei[b]						
AV %	1.423	.1671	0.668	.5126	−0.364	.7190
VA %	−4.912	.0000*	−2.245	.0376	−2.950	.0072
VLa %	6.149	.0000*	2.666	.0157	7.266	.0000*
VLp %	−2.757	.0107*	−2.459	.0243	−3.864	.0008*
VPL %	−0.800	.4314	−0.793	.4383	−0.365	.7184
Pul %	−5.376	.0000*	−4.000	.0008*	−4.163	.0004*
LGN %	−1.891	.0702	−1.509	.1485	−1.972	.0608

Table 6. Continued

	MRI1 vs. MRI2 Paired *t* Test					
	CON		FAE		FAS	
	t	*p*	*t*	*p*	*t*	*p*
MGN %	−2.159	.0406	−2.172	.0435	0.158	.8755
CM %	3.188	.0038*	0.595	.5591	2.780	.0106
MD %	2.989	.0062*	−1.536	.1420	0.190	.8510

*Indicates $p \leq .05$ corrected p value.

AV, anterior ventral nucleus; CM, centromedian; CON, control; FAE, fetal alcohol exposure; FAS, fetal alcohol syndrome; ICV, intracranial volume; LGN, lateral geniculate nucleus; MD, mediodorsal; MGN, medial geniculate nucleus; MRI, magnetic resonance imaging; Pul, pulvinar; VA, ventral anterior; VLa, ventral lateral anterior; VLp, ventral lateral posterior; VPL, ventral posterior lateral.

[a]Familywise Bonferroni correction for 4 comparisons with $\alpha = 0.05$, $p \leq .0125$.

[b]Familywise Bonferroni correction for 10 comparisons with $\alpha = 0.05$, $p \leq .005$.

statistical differences were attenuated, the abnormally small volumes of the thalamus and its regions (anterior and ventral) and nuclei (AV, VA, VLp, and VPL for FAS; LGN for FAE and FAS) were only partially accounted for by smaller ICVs, indicating an effect of PAE on these thalamic nuclei over and above that which is attributable to smaller total brain volume (Figure 10) [also see (7,11)]. The thalamic pattern is different from the cortical pattern previously reported in the current cohort, where group differences were mostly accounted for by ICV in cortical gray matter but less so in the white matter centrum semiovale (28). For the FAE/FAS comparisons, although the native volumes were significantly smaller in the FAS than in the FAE group, these differences were eliminated in all regions and nuclei with %ICV correction. This pattern is consistent with the characterization of the FAE and FAS categories as representing a spectrum rather than a separate classification of PAE.

Microcephaly and abnormally small head size are diagnostic for developmental disturbance including FASD and are typically measured by hand using a tape measure. Not surprisingly, measurement of ICV with MRI methods should present a more accurate measure of brain size. We found a small but significant correlation between MRI-derived ICV and hand measurement of orbitofrontal circumference in our control participants and participants with FAS, consistent with a recent study reporting that tape measurement of head circumference was a poor surrogate for brain volume measured with MRI (25). Furthermore, brain size, expressed herein as supratentorial ICV, did not change significantly in any group over 20 years [cf. (28)]. Another study that reported a departure from the stability of ICV from late adolescence to young adulthood noted an unexpected increase in head circumference measured with tape in participants with FAS and FAE, although the analysis was not a fully within-subjects comparison (37).

The presence of at least 2 orofacial dysmorphic signs is used with other signs to determine an FAS diagnosis, which is typically conducted in childhood (33,38). These and other physiognomic features diminish in detection with growth into adulthood (37,39–41) and are thus unlike the patterns that emerge in brain structural findings that indicate persistent deficits in ICV and other brain structures. An earlier study found that smaller volumes of the whole thalamus in addition to the putamen and pallidum correlated with longer philtrum in FASD even after controlling for ICV (7). In the current report, none of the dysmorphic measures correlated in the expected direction with thalamic volumes, perhaps reflecting diminishing orofacial dysmorphic features that may be asynchronous or progress in opposite directions with age-related brain changes or, alternatively, low statistical power given the sample sizes.

The functional relevance of the thalamic volume deficits was explored with correlations between regional measures and IQs in the combined FAE+FAS groups. One significant relationship emerged between the PIQ and the medial volume, which may be especially vulnerable to PAE given its midline position. In our earlier analysis of cerebellar morphology in this cohort, we observed a correlation between smaller lobule VIIB volumes and poorer PIQ scores (30). Together, these studies implicate cerebellothalamic pathways (42) as contributing to cognitive and motor skills engaged while performing PIQ subtests.

Despite its strength as a 20-year longitudinal study using MRI volumetry, this study has limitations. The pattern, amount, and timing of alcohol consumed by birth mothers were not available for correlation with our brain or orofacial dysmorphology measures, thereby precluding testing findings of another report that indicated a relationship between greater number of drinks per week during the first trimester and smaller ICV in PAE (7). That study also revealed correlations between severity of such dysmorphic signs and smaller whole-brain or regional volumes, specifically between smaller thalamic volumes and longer philtrum length (7), which we were unable to replicate. The attrition rate was about 50%, which falls in the range of other longitudinal studies [reviewed in (43)] (also see the Supplement), and attrition bias in our cohort was marked by higher IQ and educational level of the study returners than nonreturners in all 3 groups. Thus, these favorable features of the returners might have contributed to attenuated group differences in rates of declines. Furthermore, scanner resolution and

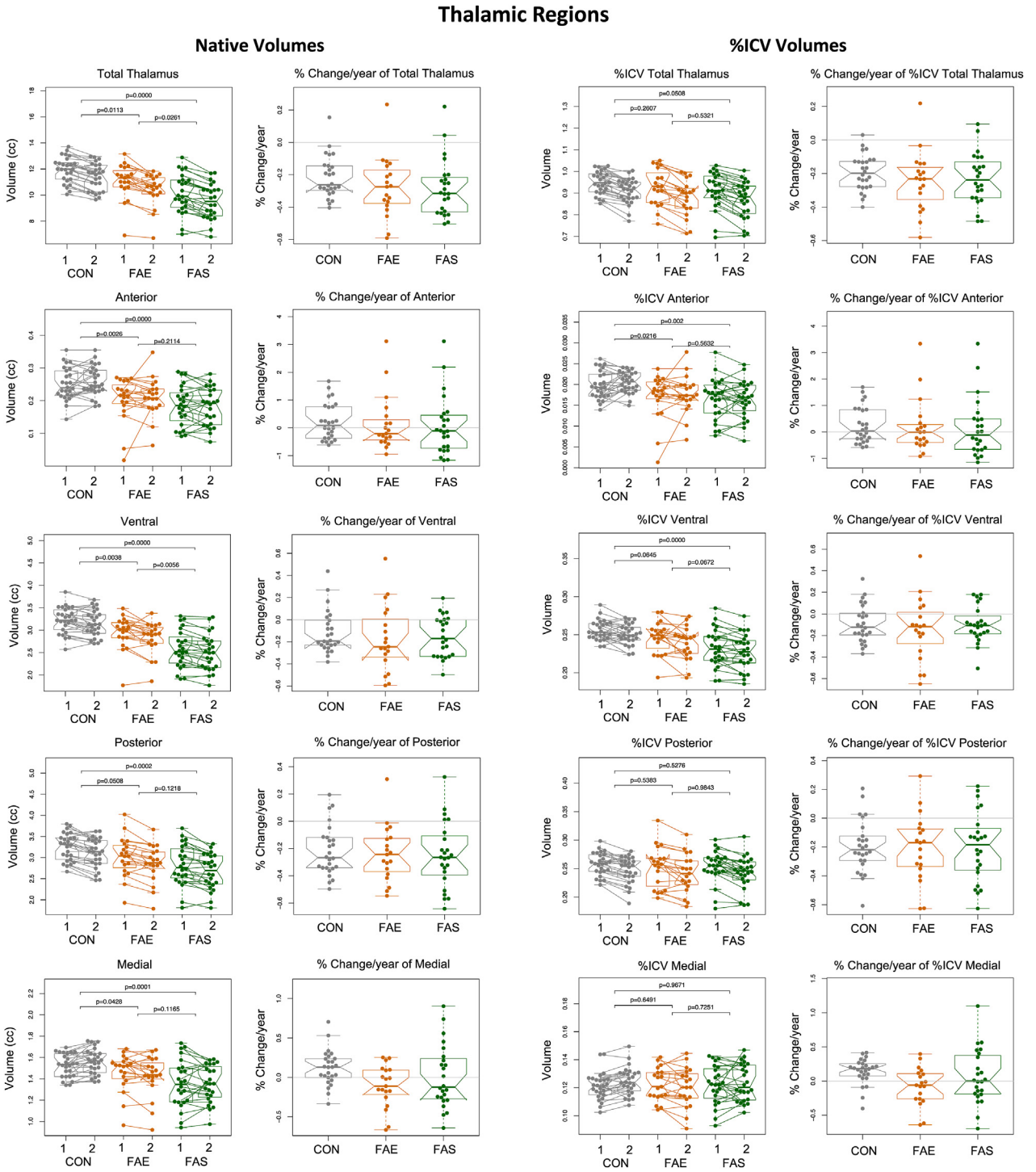

Figure 6. The left pair of plots are native volumes of thalamic regions: On the left are spaghetti plots of each participant plotted over boxplots for each regional volume at magnetic resonance imaging (MRI) 1 and MRI2. The brackets at the top with *p* values indicate statistical results of group differences. On the right are the same data expressing percentage change over the 20-year interval. The right pair of plots are percentage intracranial volume (%ICV)–adjusted volumes: On the left are spaghetti plots of each participant plotted over boxplots for each regional volume at MRI1 and MRI2. The brackets at the top with *p* values indicate the statistical results of group differences. On the right are the same data expressing percentage change over the 20-year interval. CON, control; FAE, fetal alcohol exposure; FAS, fetal alcohol syndrome.

Table 7. Longitudinal Group and Interaction *lmer* of Volumes

	Con vs. FAE		Con vs. FAS		FAE vs. FAS	
	Age × dxFAE *t*	Age × dxFAE *p*	Age × dxFAS *t*	Age × dxFAS *p*	dx × Age *t*	dx × Age *p*
ICV	−0.568	.5716	−0.918	.3621	−0.347	.7307
Native Volumes						
Regions[a]						
Anterior	−0.159	.8740	−1.206	.2318	−0.915	.3653
Ventral	−0.845	.4012	−0.138	.8907	0.626	.5344
Posterior	−0.094	.9251	−0.160	.8736	−0.085	.9329
Medial	−2.851	.0057*	−1.386	.1701	1.300	.2005
Total	−0.874	.3854	−0.523	.6029	0.311	.7576
Nuclei[b]						
AV	−0.159	.8740	−1.206	.2318	−0.915	.3653
VA	0.204	.8392	0.540	.5913	0.252	.8021
VLa	−0.601	.5498	0.449	.6549	0.909	.3682
VLp	−1.320	.1913	−0.539	.5915	0.706	.4839
VPL	−0.111	.9119	0.208	.8355	0.269	.7891
Pul	−0.115	.9087	−0.153	.8787	−0.061	.9517
LGN	−0.128	.8986	−0.384	.7018	−0.197	.8445
MGN	0.413	.6806	1.507	.1365	1.008	.3192
CM	−1.969	.0528	−0.384	.7025	1.582	.1210
MD	−2.671	.0094	−1.398	.1667	1.130	.2646
%ICV-Corrected Volumes						
Regions[a]						
Anterior %	−0.089	.9291	−1.150	.2539	−0.918	.3638
Ventral %	−0.712	.4789	0.105	.9166	0.704	.4855
Posterior %	−0.135	.8931	0.068	.9457	0.162	.8717
Medial %	−2.511	.0143	−0.661	.5110	1.547	.1290
Total %	−0.917	.3623	−0.429	.6691	0.422	.6753
Nuclei[b]						
AV %	−0.089	.9291	−1.150	.2539	−0.918	.3638
VA %	0.254	.7999	0.611	.5431	0.265	.7921
VLa %	0.064	.9493	1.357	.1789	1.075	.2876
VLp %	−1.253	.2143	−0.454	.6509	0.696	.4903
VPL %	0.117	.9074	0.356	.7226	0.215	.8307
Pul %	−0.159	.8744	0.019	.9851	0.139	.8898
LGN %	−0.028	.9779	−0.131	.8963	−0.004	.9965
MGN %	0.412	.6813	1.738	.0865	1.214	.2312
CM %	−1.605	.1127	0.209	.8347	1.767	.0840
MD %	−2.365	.0207	−0.776	.4401	1.331	.1900

*Indicates $p \leq .05$ corrected p value.

AV, anterior ventral nucleus; CM, centromedian; CON, control; dx, diagnosis; FAE, fetal alcohol exposure; FAS, fetal alcohol syndrome; ICV, intracranial volume; LGN, lateral geniculate nucleus; MD, mediodorsal; MGN, medial geniculate nucleus; Pul, pulvinar; VA, ventral anterior; VLa, ventral lateral anterior; VLp, ventral lateral posterior; VPL, ventral posterior lateral.

[a]Familywise Bonferroni correction for 4 comparisons with $\alpha = 0.05$, $p \leq .0125$.

[b]Familywise Bonferroni correction for 10 comparisons with $\alpha = 0.05$, $p \leq .005$.

conspicuity were greater in the MRI2 than MRI1, likely explaining some differences in ICV over time because of the better ability of the later MRI system to determine the edges of the brain. Nonetheless, having control participants examined at the same time and with the same scanners as participants in the FAE and FAS groups enabled us to account for scanner differences (i.e., measurement error) in ICV by group.

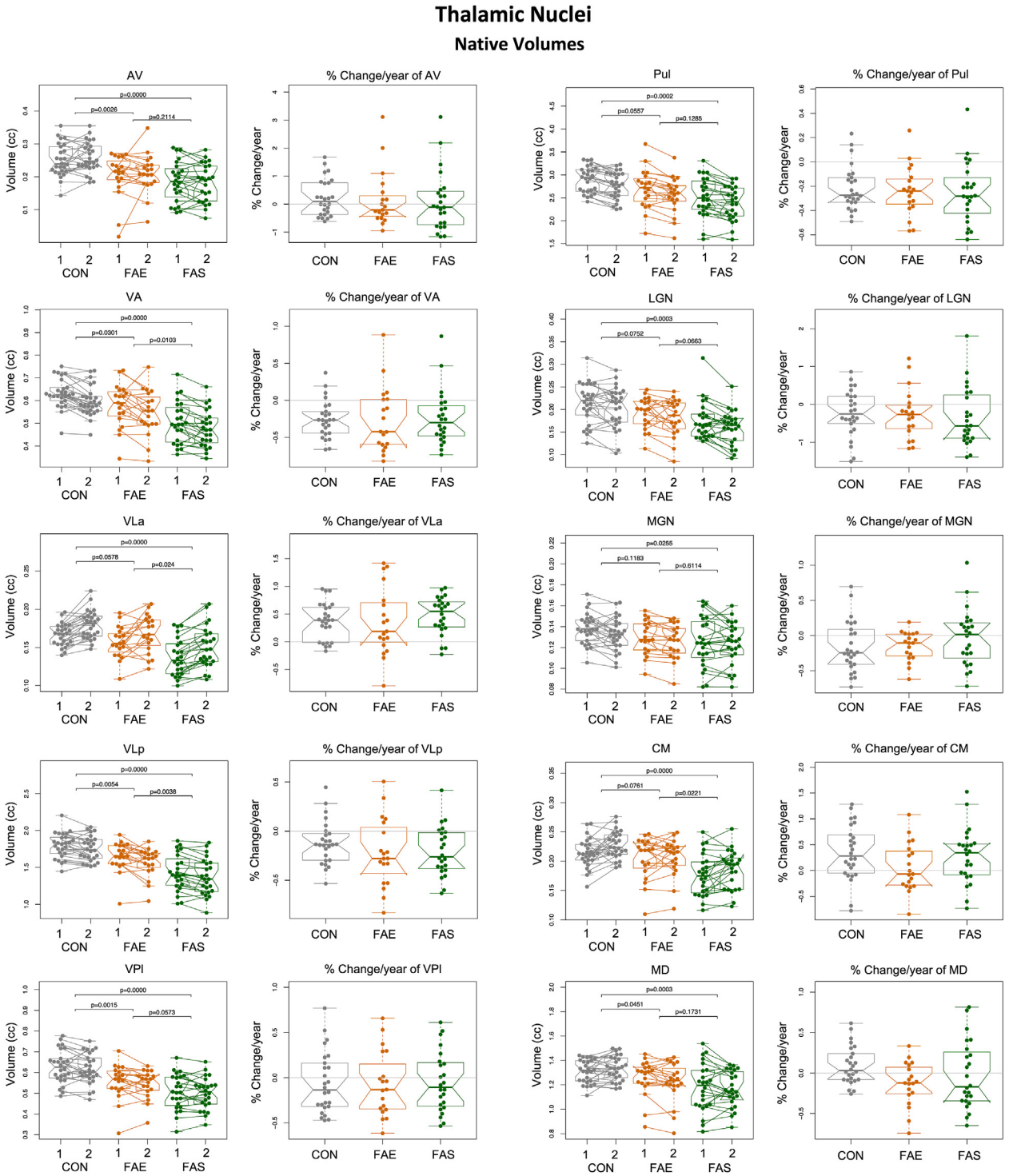

Figure 7. The left and right pairs of plots are native volumes of thalamic nuclei: On the left are spaghetti plots of each participant plotted over boxplots for each regional volume at magnetic resonance imaging (MRI) 1 and MRI2. The brackets at the top with *p* values indicate statistical results of group differences. On the right are the same data expressing percentage change over the 20-year interval. AV, anterior ventral nucleus; CM, centromedian; Con, control; FAE, fetal alcohol exposure; FAS, fetal alcohol syndrome; LGN, lateral geniculate nucleus; MD, mediodorsal; MGN, medial geniculate nucleus; Pul, pulvinar; VA, ventral anterior; VLa, ventral lateral anterior; VLp, ventral lateral posterior; VPl, ventral posterior lateral.

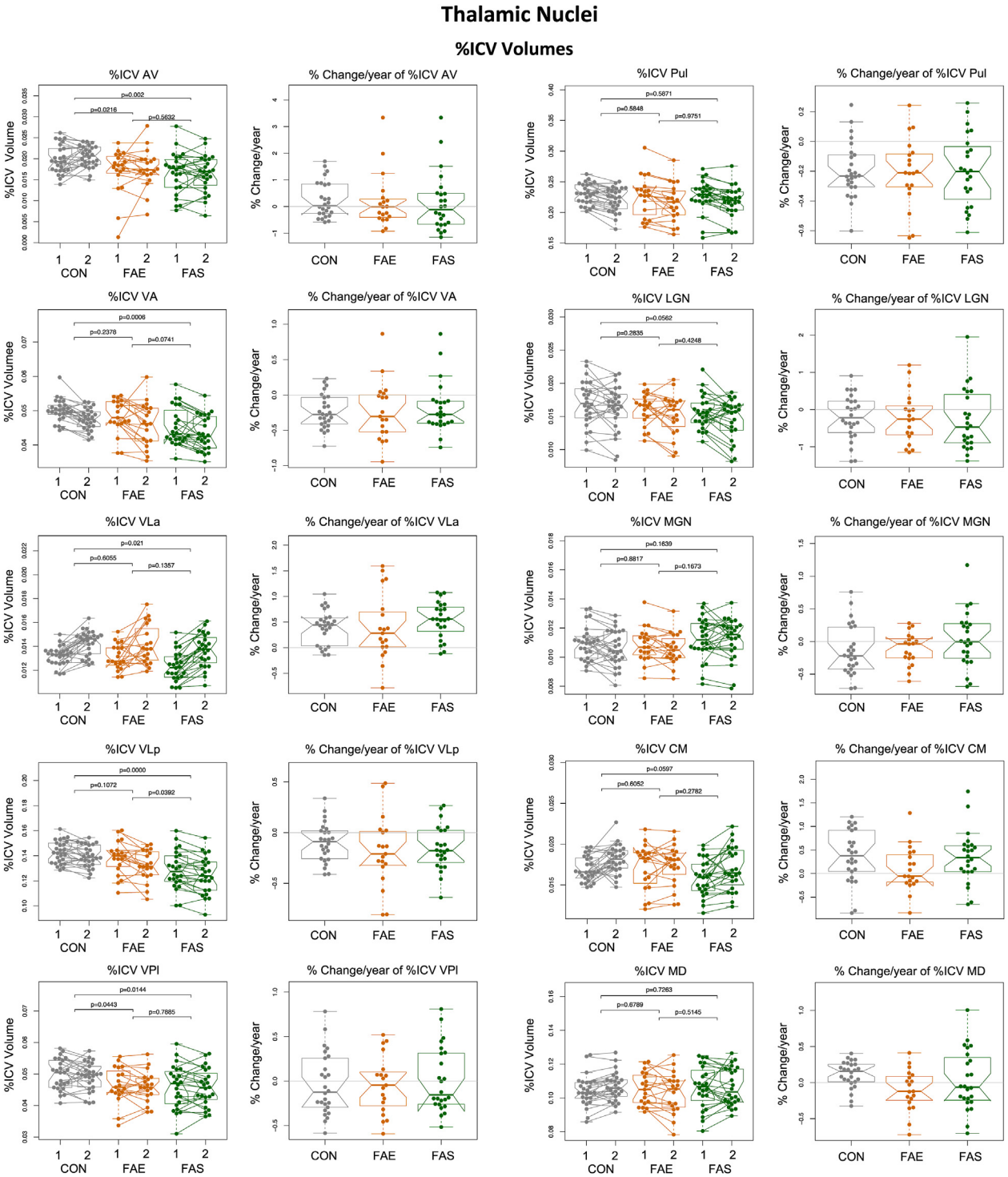

Figure 8. The left and right pairs of plots are percentage intracranial volume (%ICV)–adjusted volumes of thalamic nuclei: On the left are spaghetti plots of each participant plotted over boxplots for each nuclear volume at magnetic resonance imaging (MRI) 1 and MRI2. The brackets at the top with *p* values indicate statistical results of group differences. On the right are the same data expressing percentage change over the 20-year interval. AV, anterior ventral nucleus; CM, centromedian; Con, control; FAE, fetal alcohol exposure; FAS, fetal alcohol syndrome; LGN, lateral geniculate nucleus; MD, mediodorsal; MGN, medial geniculate nucleus; Pul, pulvinar; VA, ventral anterior; VLa, ventral lateral anterior; VLp, ventral lateral posterior; VPI, ventral posterior lateral.

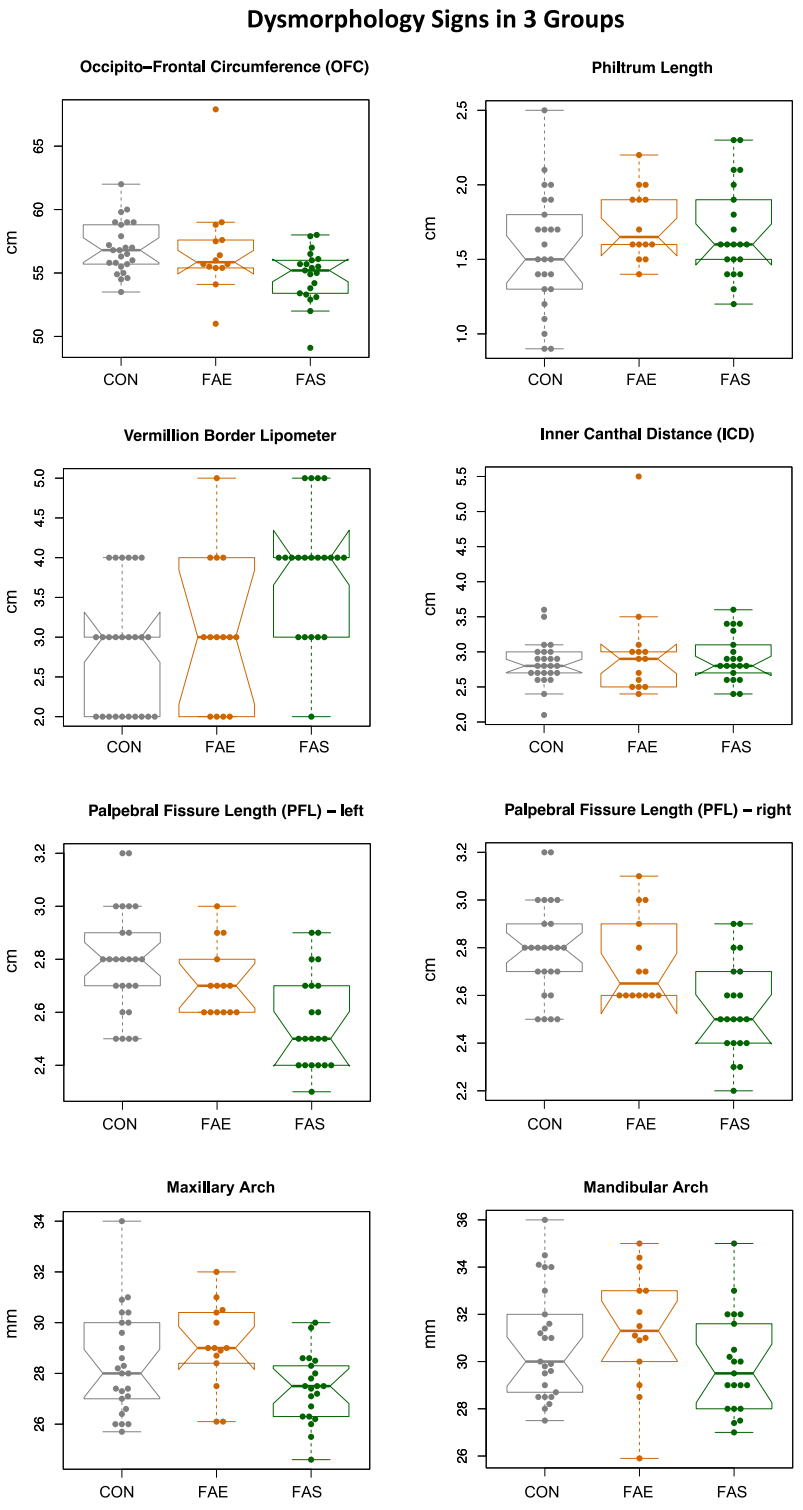

Figure 9. Bee swarm boxplots of dysmorphology signs at the second magnetic resonance imaging scan. CON, control; FAE, fetal alcohol exposure; FAS, fetal alcohol syndrome.

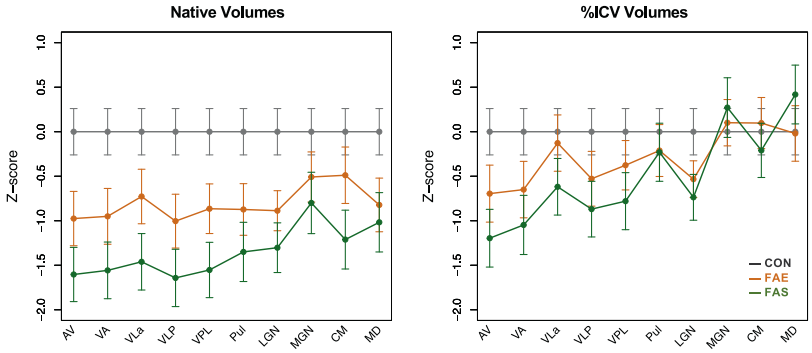

Figure 10. Profiles of native (left) and percentage intracranial volume (%ICV)–adjusted (right) volumes of each thalamic nucleus expressed as *z* scores based on control values; error bars are ±2 SEMs, that is, the 95% CI for each mean value. AV, anterior ventral nucleus; CM, centromedian; Con, control; FAE, fetal alcohol exposure; FAS, fetal alcohol syndrome; LGN, lateral geniculate nucleus; MD, mediodorsal; MGN, medial geniculate nucleus; Pul, pulvinar; VA, ventral anterior; VLa, ventral lateral anterior; VLp, ventral lateral posterior; VPl, ventral posterior lateral.

Conclusions

This longitudinal analysis is unique in measuring regional thalamic volumes over a 20-year span and revealing deficit stability in the FAE and FAS groups without accelerated decline or improvement with age that followed the same pattern observed in the control group. Despite parallel aging functions in all 3 groups, ICV adjustment for brain size yielded enduring volume deficits localized to the anterior and ventral thalamic nuclei, thereby differing from the remaining thalamic nuclei and cortical brain structures for which local volume deficits were minimized with ICV adjustment. However, it is still to be determined whether the persistent volume deficits of the anterior and ventral nuclei underlie a subset of known life-long functional impairments and whether that constellation of thalamic structures affected by exposure to prenatal alcohol will be selectively vulnerable to later-life aging.

ACKNOWLEDGMENTS AND DISCLOSURES

This research was supported by the National Institute on Alcohol Abuse and Alcoholism (Grant Nos. AA010723 [to EVS], AA021697 [to KMP], AA014811 [to EPR], and AA026994 [to EPR]) and the National Institute on Drug Abuse (Grant No. DA057567 [to KMP]). The original funding that supported participant recruitment, diagnosis, clinical interview and testing, and MRI scanning, conducted under the direction of Drs. Ann P. Streissguth, Fred L. Bookstein, P.D. Sampson, and P.D. Connor, was from the National Institutes of Health (Grant No. AA010836 [to principal investigator, Ann P. Streissguth] and GM03725 [to principal investigator, Fred L. Bookstein]).

All authors contributed significantly to this research project.

We thank Drs. Streissguth, Bookstein, Sampson, and Connor because only through their generosity in sharing their carefully collected and archived data could the analyses presented herein have been conducted. We also thank Dr. Therese Grant, who was instrumental in providing the data to us. We would also like to extend special thanks to the study participants who generously responded to our invitation to partake in this study after a 20-year period.

The data will be made available upon request by responsible users.

The authors report no biomedical financial interests or potential conflicts of interest.

ARTICLE INFORMATION

From the Center for Health Sciences, SRI International, Menlo Park, California (AP); Department of Psychiatry & Behavioral Sciences, Stanford University School of Medicine, Stanford, California (AP, EVS, KMP); Department of Radiology, UMass Chan Medical School, Worcester, Massachusetts (MS); Department of Psychiatry, University of California, San Diego, La Jolla, California (AB-G); Department of Psychiatry and Behavioral Sciences, University of Washington, Seattle, Washington (SAS); and Department of Psychology, San Diego State University, San Diego, California (EPR).

Address correspondence to Edith V. Sullivan, Ph.D., at edie@stanford.edu.

Received Feb 26, 2025; revised Apr 7, 2025; accepted Apr 8, 2025.

Supplementary material cited in this article is available online at https://doi.org/10.1016/j.bpsc.2025.04.002.

REFERENCES

1. May PA, Chambers CD, Kalberg WO, Zellner J, Feldman H, Buckley D, *et al.* (2018): Prevalence of fetal alcohol spectrum disorders in 4 US communities. JAMA 319:474–482.
2. Wozniak JR, Riley EP, Charness ME (2019): Clinical presentation, diagnosis, and management of fetal alcohol spectrum disorder. Lancet Neurol 18:760–770.
3. Sulik KK (2005): Genesis of alcohol-induced craniofacial dysmorphism. Exp Biol Med (Maywood) 230:366–375.
4. Bookstein FL, Sampson PD, Connor PD, Streissguth AP (2002): Midline corpus callosum is a neuroanatomical focus of fetal alcohol damage. Anat Rec 269:162–174.
5. Bookstein FL, Sampson PD, Streissguth AP, Connor PD (2001): Geometric morphometrics of corpus callosum and subcortical structures in the fetal-alcohol-affected brain. Teratology 64:4–32.
6. Donald KA, Eastman E, Howells FM, Adnams C, Riley EP, Woods RP, *et al.* (2015): Neuroimaging effects of prenatal alcohol exposure on the developing human brain: A magnetic resonance imaging review. Acta Neuropsychiatr 27:251–269.
7. Roussotte FF, Sulik KK, Mattson SN, Riley EP, Jones KL, Adnams CM, *et al.* (2012): Regional brain volume reductions relate to facial dysmorphology and neurocognitive function in fetal alcohol spectrum disorders. Hum Brain Mapp 33:920–937.
8. Candelaria-Cook FT, Schendel ME, Flynn L, Cerros C, Kodituwakku P, Bakhireva LN, *et al.* (2022): Decreased resting-state alpha peak frequency in children and adolescents with fetal alcohol spectrum disorders or prenatal alcohol exposure. Dev Cogn Neurosci 57:101137.
9. Mattson SN, Riley EP, Jernigan TL, Ehlers CL, Delis DC, Jones KL, *et al.* (1992): Fetal alcohol syndrome: A case report of neuropsychological, MRI and EEG assessment of two children. Alcohol Clin Exp Res 16:1001–1003.
10. Nardelli A, Lebel C, Rasmussen C, Andrew G, Beaulieu C (2011): Extensive deep gray matter volume reductions in children and adolescents with fetal alcohol spectrum disorders. Alcohol Clin Exp Res 35:1404–1417.
11. Treit S, Lebel C, Baugh L, Rasmussen C, Andrew G, Beaulieu C (2013): Longitudinal MRI reveals altered trajectory of brain development during childhood and adolescence in fetal alcohol spectrum disorders. J Neurosci 33:10098–10109.
12. Mattson SN, Riley EP, Jernigan TL, Garcia A, Kaneko WM, Ehlers CL, Jones KL (1994): A decrease in the size of the basal ganglia following prenatal alcohol exposure: A preliminary report. Neurotoxicol Teratol 16:283–289.

13. Archibald SL, Fennema-Notestine C, Gamst A, Riley EP, Mattson SN, Jernigan TL (2001): Brain dysmorphology in individuals with severe prenatal alcohol exposure. Dev Med Child Neurol 43:148–154.
14. Aggleton JP, Pralus A, Nelson AJD, Hornberger M (2016): Thalamic pathology and memory loss in early Alzheimer's disease: Moving the focus from the medial temporal lobe to Papez circuit. Brain 139:1877–1890.
15. Segobin S, Haast RAM, Kumar VJ, Lella A, Alkemade A, Bach Cuadra M, *et al.* (2024): A roadmap towards standardized neuroimaging approaches for human thalamic nuclei. Nat Rev Neurosci 25:792–808.
16. Dum RP, Levinthal DJ, Strick PL (2009): The spinothalamic system targets motor and sensory areas in the cerebral cortex of monkeys. J Neurosci 29:14223–14235.
17. Vidal JP, Danet L, Péran P, Pariente J, Bach Cuadra M, Zahr NM, *et al.* (2024): Robust thalamic nuclei segmentation from T_1-weighted MRI using polynomial intensity transformation. Brain Struct Funct 229:1087–1101.
18. Choi EY, Tian L, Su JH, Radovan MT, Tourdias T, Tran TT, *et al.* (2022): Thalamic nuclei atrophy at high and heterogenous rates during cognitively unimpaired human aging. Neuroimage 262:119584.
19. Pfefferbaum A, Zahr NM, Sassoon SA, Fama R, Saranathan M, Pohl KM, Sullivan EV (2024): Aging, HIV infection, and alcohol exert synergist effects on regional thalamic volumes resulting in functional impairment. NeuroImage Clin 44:103684.
20. Pfefferbaum A, Sullivan EV, Zahr NM, Pohl KM, Saranathan M (2023): Multi-atlas thalamic nuclei segmentation on standard T1-weighed MRI with application to normal aging. Hum Brain Mapp 44:612–628.
21. Mattson SN, Bernes GA, Doyle LR (2019): Fetal alcohol spectrum disorders: A review of the neurobehavioral deficits associated with prenatal alcohol exposure. Alcohol Clin Exp Res 43:1046–1062.
22. Moore EM, Riley EP (2015): What happens when children with fetal alcohol spectrum disorders become adults? Curr Dev Disord Rep 2:219–227.
23. Moore EM, Xia Y (2021): Neurodevelopmental trajectories following prenatal alcohol exposure. Front Hum Neurosci 15:695855.
24. Gautam P, Lebel C, Narr KL, Mattson SN, May PA, Adnams CM, *et al.* (2015): Volume changes and brain-behavior relationships in white matter and subcortical gray matter in children with prenatal alcohol exposure. Hum Brain Mapp 36:2318–2329.
25. Gimbel BA, Roediger DJ, Ernst AM, Anthony ME, Mueller BA, de Water E, *et al.* (2024): Normative magnetic resonance imaging data increase the sensitivity to brain volume abnormalities in the classification of fetal alcohol spectrum disorder. J Pediatr 266:113868.
26. Zhou D, Rasmussen C, Pei J, Andrew G, Reynolds JN, Beaulieu C (2018): Preserved cortical asymmetry despite thinner cortex in children and adolescents with prenatal alcohol exposure and associated conditions. Hum Brain Mapp 39:72–88.
27. Pfefferbaum A, Kwon D, Brumback T, Thompson WK, Cummins K, Tapert SF, *et al.* (2018): Altered brain developmental trajectories in adolescents after initiating drinking. Am J Psychiatry 175:370–380.
28. Pfefferbaum A, Sullivan EV, Pohl KM, Bischoff-Grethe A, Stoner SA, Moore EM, Riley EP (2023): Brain volume in fetal alcohol spectrum disorders over a 20-year span. JAMA Netw Open 6:e2343618.
29. Inkelis SM, Moore EM, Bischoff-Grethe A, Riley EP (2020): Neurodevelopment in adolescents and adults with fetal alcohol spectrum disorders (FASD): A magnetic resonance region of interest analysis. Brain Res 1732:146654.
30. Sullivan EV, Moore EM, Lane B, Pohl KM, Riley EP, Pfefferbaum A (2020): Graded cerebellar lobular volume deficits in adolescents and young adults with fetal alcohol spectrum disorders (FASD). Cereb Cortex 30:4729–4746.
31. Bookstein FL, Streissguth AP, Sampson PD, Connor PD, Barr HM (2002): Corpus callosum shape and neuropsychological deficits in adult males with heavy fetal alcohol exposure. Neuroimage 15:233–251.
32. Wechsler D (1981): Wechsler Adult Intelligence Scale-Revised. New York: The Psychological Corporation.
33. Hoyme HE, Kalberg WO, Elliott AJ, Blankenship J, Buckley D, Marais AS, *et al.* (2016): Updated clinical guidelines for diagnosing fetal alcohol spectrum disorders. Pediatrics 138:e20154256.
34. Suttie M, Wozniak JR, Parnell SE, Wetherill L, Mattson SN, Sowell ER, *et al.* (2018): Combined face-brain morphology and associated neurocognitive correlates in fetal alcohol spectrum disorders. Alcohol Clin Exp Res 42:1769–1782.
35. Fama R, Sassoon SA, Müller-Oehring EM, Saranathan M, Pohl KM, Zahr NM, *et al.* (2024): Anterior and posterior thalamic volumes differentially correlate with memory, attention, and motor processes in HIV infection and alcohol use disorder comorbidity. Brain Res Bull 217:111085.
36. R core Team (2019): R: A Language and Environment for Statistical Computing. Vienna, Austria: R Foundation for Statistical Computing. https://www.R-project.org/.
37. Spohr HL, Willms J, Steinhausen HC (2007): Fetal alcohol spectrum disorders in young adulthood. J Pediatr 150:175–179.
38. Hoyme HE, May PA, Kalberg WO, Kodituwakku P, Gossage JP, Trujillo PM, *et al.* (2005): A practical clinical approach to diagnosis of fetal alcohol spectrum disorders: Clarification of the 1996 institute of medicine criteria. Pediatrics 115:39–47.
39. Blanck-Lubarsch M, Dirksen D, Feldmann R, Hohoff A (2023): A systematic review: Facial, dental and orthodontic findings and orofacial diagnostics in patients with FASD. Front Pediatr 11:1169570.
40. Chong Y, Dong R, Liu X, Wang X, Yu N, Long X (2021): Stereophotogrammetry to reveal age-related changes of labial morphology among Chinese women aging from 20 to 60. Skin Res Technol 27:41–48.
41. Ramaut L, Tonnard P, Verpaele A, Verstraete K, Blondeel P (2019): Aging of the upper lip: Part I: A retrospective analysis of metric changes in soft tissue on magnetic resonance imaging. Plast Reconstr Surg 143:440–446.
42. Heck DH, Fox MB, Correia Chapman B, McAfee SS, Liu Y (2023): Cerebellar control of thalamocortical circuits for cognitive function: A review of pathways and a proposed mechanism. Front Syst Neurosci 17:1126508.
43. Stange JP, Jenkins LM, Bessette KL, Kling LR, Bark JS, Shepard R, *et al.* (2018): Predictors of attrition in longitudinal neuroimaging research: Inhibitory control, head movement, and resting-state functional connectivity. Brain Connect 8:527–536.